Synthesis of Stilbene and Chalcone Inhibitors of Influenza A Virus by SBA-15 Supported Hoveyda-Grubbs Metathesis

Bruno Mattia Bizzarri [1,*]**, Angelica Fanelli** [1]**, Davide Piccinino** [1]**, Marta De Angelis** [2]**, Camilla Dolfa** [2]**, Anna Teresa Palamara** [2]**, Lucia Nencioni** [2,*]**, Claudio Zippilli** [1]**, Marcello Crucianelli** [3] **and Raffaele Saladino** [1]

[1]   Department of Ecology and Biology, University of Tuscia, 01100 Viterbo, Italy;
     fanelli.angelica@gmail.com (A.F.); d.piccinino@unitus.it (D.P.); zippillic@unitus.it (C.Z.);
     saladino@unitus.it (R.S.)

[2]   Department of Public Health and Infectious Diseases, Laboratory affiliated to Istituto Pasteur Italia,
     Fondazione Cenci Bolognetti, Sapienza University of Rome, 00185 Rome, Italy;
     marta.deangelis@uniroma1.it (M.D.A.); camilla.dolfa@uniroma1.it (C.D.);
     annateresa.palamara@uniroma1.it (A.T.P.)

[3]   Department of Physical and Chemical Sciences, University of L'Aquila, 67100 L'Aquila, Italy;
     marcello.crucianelli@univaq.it

*   Correspondence: bm.bizzarri@unitus.it (B.M.B.); lucia.nencioni@uniroma1.it (L.N.);
     Tel.: +39-0761357239 (B.M.B.); Tel.: +39-0649914608 (L.N.)

Abstract: Stilbene and chalcone derivatives with biological activity against influenza A virus have been synthesized by self-, cross-, and ring-closing metathesis procedures. The reactions were performed under environmentally friendly conditions using the second generation Hoveyda-Grubbs catalyst Aquamet SiPr after immobilization on Santa Barbara Amorphous mesoporous silicate SBA-15. Irrespective from the experimental conditions, the heterogeneous catalyst showed activity and selectivity comparable than the homogeneous counterpart for at least six successive runs without appreciable leaching of the active species. An appreciable antiviral activity against influenza A virus for some of the novel derivatives were observed, mainly involving the early stage of the virus-replication life-cycle.

1. Introduction

Influenza represents a severe threat worldwide, causing large epidemics and pandemics responsible for thousands of deaths and hospitalization every year [1]. The influenza A virus is an enveloped virus belonging to the *Orthomyxoviridae* family, characterized by a segmented single-stranded RNA genome [2]. During the infection, eight viral RNA segments associated with the nucleoprotein (NP) and the viral RNA-dependent RNA polymerase (RdRp) complex are transported to the host-cell nucleus, where they undergo replication and transcription, followed by release into the cytosol to be assembled into progeny virions [3]. Present-day, three families of antiviral compounds have been developed against influenza A virus. The first one blocks the ion-channel activity of the viral Matrix (M2) protein, which is mainly required for virus uncoating [4]. The second family includes inhibitors of the viral glycoprotein Neuraminidase (NA), which allows the release of viral particles from infected cells [5]. The last one includes compounds active against the polymerase complex, two of them,

baloxavir marboxil and favirapir being recently licensed in Japan and United States. The efficacy of these antiviral compounds, however, is often limited by toxicity and the almost inevitable selection of drug-resistant viral mutants [6]. Thus, new antiviral agents are required to efficiently inhibit influenza viruses.

Stilbenes and chalcones are natural compounds characterized by several biological activities, including defense mechanisms in plants [7], fungicidal activity [8], antioxidant [9], chemopreventive [10] and cardioprotective effects [11], atherosclerosis [12], neurodegeneration [13], obesity [14] and diabetes control [15], and antimicrobial [16] and anticancer activities [17]. Analysis and reviews of the role of stilbenes in viral therapy [18], such as the inhibition of herpes simplex-1 (HSV-1), herpes simplex-2 (HSV-2) [19], respiratory syncytial (RSV) [20], human immunodeficiency (HIV) [21], varicella-zoster [22], and hepatitis C viruses [23], have been reported, including the activity against Influenza viruses [24]. In this latter case, the antiviral activity was associated with the block of nuclear-cytoplasmic translocation of viral ribonucleoproteins, as well as, to tuning of the intracellular redox state of the cell [6]. The metathesis is a general and efficient strategy for the synthesis of stilbene and chalcone derivatives [25,26]. For example, the Hoveyda-Grubbs second generation of ruthenium reagents [27] has been applied in the metathesis [28,29] of eugenol [30] to yield a large panel of stilbenes bearing acrylate, acrylonitrile and acrylamide side-chains [31,32]. The self-metathesis of eugenol with Grubbs catalysts also afforded intermediates for the preparation of renewable thermosetting bis(cyanate) ester resins [33].

In the last years, environmental concerns prompted towards the design and development of heterogeneous metathesis catalysts by immobilization of active ruthenium species on eco-compatible and stable supports [34,35]. This procedure improved the stability of ruthenium species expanding the functional group tolerances with respect to homogeneous counterpart and offered a great solution for catalyst recovery problems [36]. Santa Barbara Amorphous mesoporous silicate SBA-15 has been applied for the immobilization of Hoveyda-Grubbs catalysts in both ring-closing metathesis and homo-metathesis processes [37]. SBA-15 is characterized by uniform pore size (4.6–30 nm), well-defined pore structure and size-distribution, high surface area, high thermal stability and capability to support a large panel of active species [38,39]. The preparation, structural characterization and application of mesoporous molecular sieves as advanced support for olephin metathesis catalyst is reviewed [40,41]. Different examples of Hoveyda-Grubbs catalysts supported on SBA-15 have been reported, even if they have been scarcely applied in the synthesis bioactive compounds [42,43]. We describe here the synthesis of stilbene and chalcone derivatives by use of the second-generation ruthenium Hoveyda-Grubbs catalyst Aquamet SIPr (ASIPr) after immobilization on SBA-15 (Scheme 1). Self-metathesis, mixed olefin metathesis and ring-closing metathesis procedures have been applied, starting from a large panel of allyl and vinyl-benzene substrates.

Scheme 1. Aquamet SIPr (ASIPr) supported on SBA-15 as catalysts for metathesis reaction.

The novel derivatives showed an appreciable antiviral activity against influenza A virus. In the case of the most active compound, a detailed investigation of the molecular effect on infected cells is reported.

2. Results

2.1. ASIPr/SBA-15 Catalyzed Synthesis of Stilbene Derivatives

The second-generation ruthenium Hoveyda-Grubbs catalyst Aquamet SIPr (ASIPr) [44] was immobilized on SBA-15 by applying the impregnation method reported in ref [42]. Briefly, ASIPr (10 mg) in dry CH_2Cl_2 (10 mL) was added to SBA-15 (1.0 g) in a Schlenk tube under argon atmosphere

at 25 °C for 4 h. The supernatant was removed by filtration on GH-polypro hydrophilic membranes (47 mm 0.2 μm) and the solid residue was recovered, washed with dry CH_2Cl_2, and dried under vacuum to yield ASIPr/SBA-15 (Figure 1).
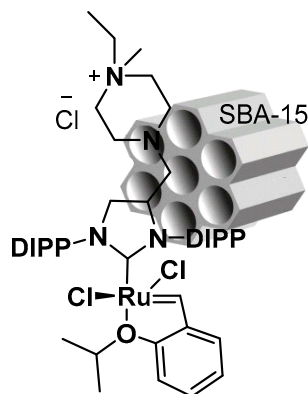

Figure 1. Schematic representation of ASIPr/SBA-15 Hoveyda-Grubbs catalyst.

Nitrogen adsorption isotherms showed that SBA-15 retained the mesoporous structure and pore size distribution after the loading of ASIPr, in accordance with data previously reported [42]. BET surface area, void volume and average pore diameters of SBA-15 and ASIPr/SBA-15 are showed in Table 1. The related isotherms are in SI#1. The slight decrease of the mesopore volume (from 1.12 to 0.98 cm^3/g) and BET surface area (from 861 to 693 m^2/g) confirmed the loading of the catalyst. Moreover, the variation in the average value of the pore diameter in ASIPr/SBA-15 with respect to native SBA-15 (from 5.5 to 5.4) suggested the presence of the complex mainly inside the pores.

Table 1. Textural parameters of SBA-15 and ASIPr/SBA-15 Hoveyda-Grubbs catalyst.

	BET Surface Area (m^2/g)	Void Volume (cm^3/g)	Average Pore Diameter (nm)
SBA-15	861	1.12	5.5
ASIPr/SBA-15	693	0.98	5.4

Inductively coupled plasma mass spectrometry (ICP-MS) analysis of ASIPr/SBA-15 showed the presence of 1.0 wt/% of ruthenium, suggesting the occurrence of the quantitative immobilization of the active species on SBA-15. This data was in accordance with results previously reported [42]. The Structural integrity of SBA-15 after deposition of ASIPr was confirmed by Scanning Electron Microscopy (SEM) analysis (Figure 2). Particles of regular shape with an average diameter of 1.0 ± 0.1 μm and homogeneous distribution were observed before and after the loading procedure.
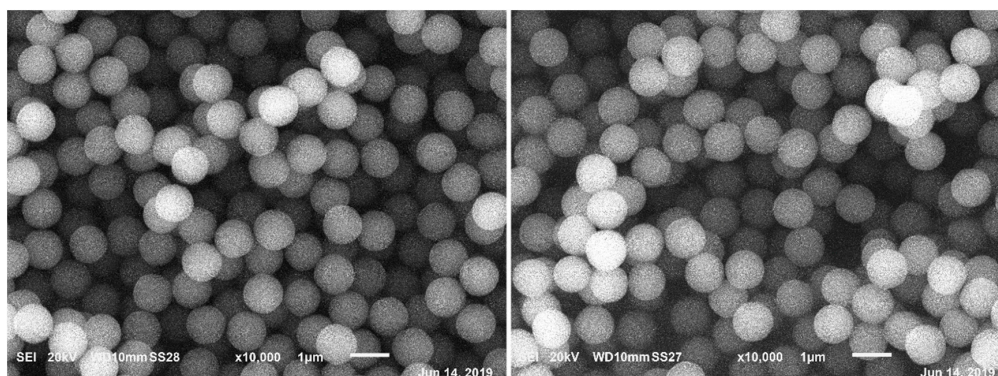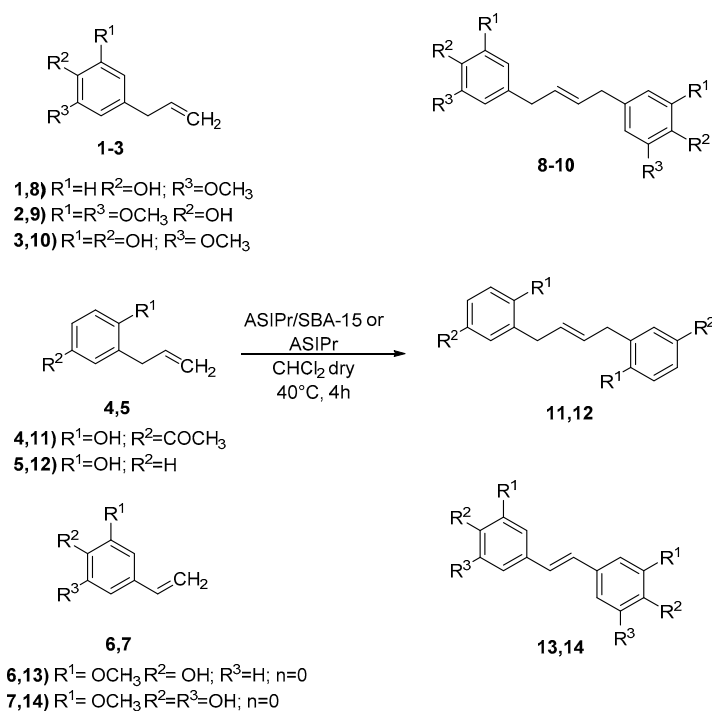

Figure 2. Scanning Electron Microscopy of SBA-15 before (**left** panel) and after (**right** panel) the immobilization of ASIPr.

Initially, ASIPr/SBA-15 was used for the self-metathesis of allyl- and vinyl-benzene derivatives, including eugenol **1**, 4-allyl-2,6-dimethoxyphenol **2**, 4-allyl-2-hydroxy-6-methoxyphenol **3**, 3-allyl-4-hydroxyacetophenone **4**, 2-allyl-phenol **5**, 4-vinyl-2-methoxy-phenol (4-vinyl-guaiacol) **6**, and 4-vinyl-2-hydroxy-6-methoxy-phenol **7**. The reactions were performed by treating the appropriate substrate (0.6 mmol) in dry CH_2Cl_2 (5.0 mL) with a catalytic amount of ASIPr/SBA-15 (2.0×10^{-3} mmol of immobilized Ru, corresponding to 8.8 mg of heterogenous catalyst) of under argon atmosphere at 40 °C for 4 h.

The self-metathesis of compound **1** and **6** were performed with ASIPr as a reference. Irrespective to experimental conditions, the stilbene derivatives **8–14** (Scheme 2) were obtained from acceptable to high yield beside to few amounts of the unreacted substrate (Table 1, entries 2–9). The reaction proceeded with high selectivity to afford trans-isomers as evaluated by ^{1}H NMR analysis (SI#2), in accordance with the known regioselectivity pattern previously reported for Hoveyda-Grubbs catalysts [45] ASIPr/SBA performed in a way similar to ASIPr alone in the self-metathesis of eugenol **1**, suggesting the complete retention of the reactivity of ruthenium after the immobilization on SBA-15 (Table 2, entry 1 versus entry 2). The presence of the OH moiety in the *ortho*-position of the substrate with respect to the side-chain, as in the case of compounds **4** and **5**, significantly decreased the yield of the reaction (Table 2, entries 5–6 versus entries 2–4), as a consequence of the unfavorable electron-donating effect associated to the oxygen atom [46]. At contrary, the reduction of the length of the olefin side-chain in compounds **6–7** (that are vinyl-like derivatives) increased both conversion of substrate and yield of stilbene derivatives **13–14** (Table 2, entries 8–9), ASIPr/SBA performing as the homogeneous counterpart (Table 2, entry 7 versus entries 8–9). Next, ASIPr/SBA-15 was applied in the cross-olefin metathesis of compounds **2**, **5**, and **3**, **15–16**, respectively. The reaction was performed under previously reported experimental conditions using equimolar amount of the two reagents to afford stilbene derivatives **17–19** (Scheme 3). As a general trend, the higher yield of the desired product was obtained with substrates deprived of the OH substituent in the *ortho*-position with respect to the olefin side-chain, confirming the detrimental electronic effect previously observed in the case of the self-metathesis reactions (Table 1, entry 11 versus entries 12–13).

1,8) R[1]=H R[2]=OH; R[3]=OCH$_3$
2,9) R[1]=R[3]=OCH$_3$ R[2]=OH
3,10) R[1]=R[2]=OH; R[3]=OCH$_3$

4,11) R[1]=OH; R[2]=COCH$_3$
5,12) R[1]=OH; R[2]=H

6,13) R[1]=OCH$_3$ R[2]=OH; R[3]=H; n=0
**7,14)** R[1]=OCH$_3$ R[2]=R[3]=OH; n=0

Scheme 2. Self-metathesis of allyl and vinyl-benzene derivatives **1–7** in the presence of ASIPr/SBA-15 and ASIPr.

Table 2. ASIPr/SBA-15 catalyzed the synthesis of stilbene derivatives **8–14**, **18–20** and chalcones **23–24**, by self-metathesis, cross-olefin metathesis and ring-closing metathesis, respectively [a].

Entry	Substrate(s)	Catalyst	Conversion (%)	Product	Yield (%) [c]
1	**1**	ASIPr	71	**8**	48
2	**1**	ASIPr/SBA-15	70	**8**	52
3	**2**	ASIPr/SBA-15	75	**9**	56
4	**3**	ASIPr/SBA-15	68	**10**	41
5	**4**	ASIPr/SBA-15	35	**11**	18
6	**5**	ASIPr/SBA-15	27	**12**	15
7	**6**	ASIPr	88	**13**	70
8	**6**	ASIPr/SBA-15	93	**13**	73
9	**7**	ASIPr/SBA-15	95	**14**	75
10	**2, 3** [b]	ASIPr	91	**17(9)** [c] **(10)** [c]	68(12)(9)
11	**2, 3** [b]	ASIPr/SBA-15	90	**17(9)** [c] **(10)** [c]	65 (11)(10)
12	**2, 15** [b]	ASIPr/SBA-15	45	**18(9)** [c]	25(16)
13	**5, 15** [b]	ASIPr/SBA-15	30	**19(12)** [c]	22(4)
14	**20**	ASIPr	60	**22**	21
15	**20**	ASIPr/SBA-15	58	**22**	24
16	**21**	ASIPr/SBA-15	55	**23**	21

[a] Reactions were performed treating the appropriate substrate (0.6 mmol) with ASIPr/SBA (2.0 wt/%) under argon atmosphere at 40 °C for 4 h. [b] Reactions performed treating equimolar amount of the appropriate substrates (0.3 mmol) with ASIPr/SBA (2.0 wt/%) under argon atmosphere at 40 °C for 4 h. Reactions were performed in triplicate. [c] Data in parentheses are referred to as self-metathesis by-products obtained during the cross-metathesis reactions. Compound 9 is the side-product deriving from the homocoupling of 2, compound 10 is the side-product deriving from the homocoupling of 3, compound 12 is the side-product deriving from the homocoupling of 5.
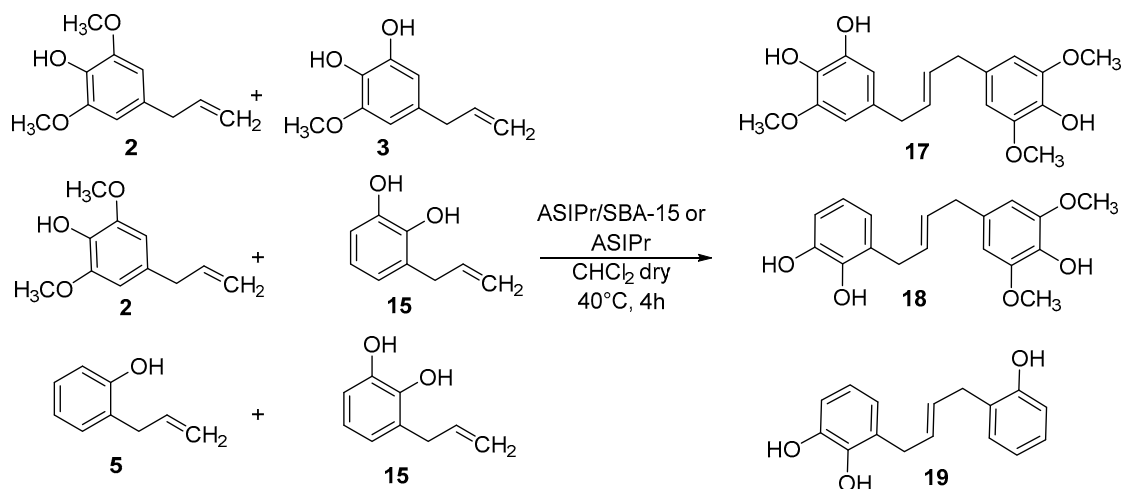
Scheme 3. Mixed olefin-metathesis of allyl-benzene derivatives **2**, **5** and **3**, **15**, **16** in the presence of ASIPr/SBA-15 and ASIPr.

Finally, ASIPr/SBA-15 was tested in the ring-closing metathesis of chalcone derivatives **20** and **21**. Compounds **20** and **21** were prepared by aldolic condensation between 4-hydroxy-3-allyl acetophenone (0.01 mol) and the appropriate aldehydes (0.01 mol) in EtOH under basic conditions (KOH, 0.3 mol) at 25 °C for 24 h [47], and then treated with ASIPr/SBA-15 (2.0 wt/%) in dry CH_2Cl_2 (5.0 mL) under argon atmosphere at 40 °C for 4 h to afford macro-cyclic chalcones **22** and **23** in acceptable yield (Scheme 4, Table 1 entries 15–16). The low mass-balance of the self, cross and ring-closing metathesis reactions suggested the occurrence of oligomerization processes to yield high molecular weight products not isolable from the reaction mixture. In the case of cross-metathesis, some homo-coupled products were also obtained as reported in Table 2. A similar reaction pathway was observed in the case of ASIPr (Table 1, entry 14).
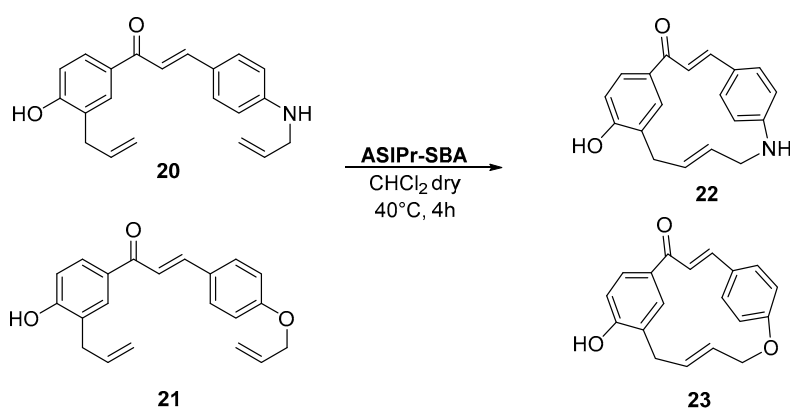
Scheme 4. Ring-closing metathesis of chalcone derivatives **23** and **24** in the presence of ASIPr/SBA-15 and ASIPr.

The recyclability of ASIPr/SBA-15 was evaluated by analysing the self-metathesis of compound **2** as a selected example. The experiment was performed by the recovery of ASIPr/SBA-15 for five runs, followed by its re-use under reported experimental conditions. Table 3 shows the conversion of substrate and yield of stilbene **9** for any run. The leaching of ruthenium in the recyclability experiments after any runs was evaluated by ICP-MS analysis of the reaction mixture after removal of the heterogeneous catalyst by filtration. As a general trend, ASIPr/SBA-15 retained the reactivity during the recycles, showing ca. 82% of the initial conversion value at the last run. Overall, 7.6% of the initial amount of ruthenium was lost during the recycles. The partial leaching of ASIPr during different runs may be responsible for the slight decrease in the conversion and yield of reactions, this leaching behavior being in accordance with data previously reported for similar catalyst.

Table 3. Recyclability of ASIPr/SBA-15 in the synthesis of stilbene derivative **6** [a].

Entry	Substrate	Conversion (%)	Yield (%)	Ru Leaching [b]
1	**2**	73	56	1.6
2	**2**	72	56	1.4
3	**2**	70	52	1.0
4	**2**	70	51	1.2
5	**2**	64	47	1.3
6	**2**	60	46	1.1

[a] Reactions were performed by recovery of ASIPr/SBA-15 for five runs and its re-use under reported experimental conditions. [b] Leaching of ruthenium expressed as % with respect to the initial amount of ASIPr.

2.2. Antioxidant Activity of Compounds **8–14** and **17–23**

The in vitro antioxidant activity of selected compounds **8–14** and **20–23** were evaluated by the analysis of the 2,2'-diphenyl picrylhydrazyl (DPPH) radical scavenging properties [48]. The DPPH activity of ascorbic acid (**AA**) and eugenol were evaluated as references. Briefly, the appropriate compounds were dissolved in EtOH (500, 250, 100, 50, and 10 μg/mL) and added to a freshly prepared DPPH solution (6×10^{-5} M in EtOH). The decrease in absorbance (518 nm) was determined at different times until the reaction reached a plateau. The kinetic was analyzed for each concentration tested, and the rate of DPPH remaining at the steady-state was estimated. This value was used to calculate the IC_{50} (defined as the concentration of substrate μg/mL that causes 50% loss of DPPH activity). Results reported As a general trend, stilbene derivatives **8–10** and **13–14** showed antioxidant activity comparable to eugenol, and higher than chalcone derivatives **20–23** (Table 4). This result was probably due to the higher radical scavenging properties of catechol with respect to the simple phenol moiety [49], associated to the better capacity of dimer species to trap an increased number of free radicals [50]. Moreover, derivatives bearing the allyl side-chain showed an antioxidant activity higher than the vinyl counterpart in the stilbene family (Table 3).

Table 4. DPPH assay of compounds **8–14** and **20–23**.

| Entry | Compound | DPPH Assay | | | | | |
| | | % Inhibition | | | | | IC50 [a] |
		500	250	100	50	10	
1	**A.A.**	99.9	97.1	92.4	79.19	4.4	13.2
2	**eugenol**	99.9	97.1	92.4	75.19	38.4	19.6
3	**8**	98.1	91.6	83.7	60.2	26.8	35.4
4	**9**	98.2	91.8	83.9	60.4	26.9	34.9
5	**10**	98.2	96.1	87.4	67.1	30.7	31.3
6	**11**	95.3	85.2	67.1	47.3	13.0	54.6
7	**12**	96.1	86.6	71.0	48.3	16.1	52.1
8	**13**	96.5	90.5	82.2	59.5	28.4	36.4
9	**14**	98.0	91.4	83.5	58.7	26.9	35.2
10	**19**	91.1	88.2	75.4	56.2	16.4	40.1
11	**20**	95.1	89.9	78.6	53.5	18.4	45.3
12	**21**	86.11	72.2	55.9	33.0	8.1	81.3
13	**22**	83.1	69.9	50.1	28.4	2.7	98.3
14	**23**	84.3	70.2	53.6	31.1	5.6	90.1

[a] concentration of substrate µg/mL that causes 50% loss of DPPH activity.

2.3. Antiviral Activity Against Influenza A Virus Replication

In the first set of experiments, the potential cytotoxicity of stilbene and chalcone derivatives was evaluated. Briefly, A549 cells were plated at concentration of 2×10^5/mL and after 24 h were treated with various concentrations (range 1–50 µg/mL) of each compound and incubated for the following 24 h. Microscopic examination and trypan blue exclusion demonstrated that most of the analyzed compounds exerted a toxic effect at the highest concentration (20–50 µg/mL) (data not shown). Similar results were obtained by evaluating the cell protein expression on cells by In-Cell Western (ICW) assay [51]. On the basis of cytotoxicity data, the concentration of 50 µg/mL was excluded and all the compounds were tested for their potential antiviral activity at concentrations causing cell viability ≥ 80%. The cells were infected with influenza A/PR8/H1N1 virus and, after viral challenge, they were treated with different concentrations of each compound (ranging from 1 to 20 µg/mL). Twenty-four hours post-infection (p.i.), viral production was quantified by haemagglutination assay (HAU) on the supernatants of infected cells. As shown in Table 5, stilbene derivatives **9** and **12**, and chalcone **22** were active against influenza A virus, showing IC50 values (50% inhibitory concentration) lesser than 15 µg/mL (Table 5, entries 2, 5, and 13, respectively). Among them, chalcone **22** was characterized by a selectivity index (that is CC50/IC50) relatively high (Table 5, entry 13). Note that stilbene **9** caused a cell proliferation at high concentrations (20 and 50 µg/mL), therefore the evaluation of its antiviral activity might be partially affected by this process.

The anti-influenza efficacy of stilbenes, such as resveratrol and its analogues, has been previously reported by our group [24,48]. In order to better identify the antiviral mechanism of chalcone **22**, we decided to study the expression of viral nucleoprotein (NP) by ICW assay and the viral RNA expression of Matrix 2 (M2), by Real-Time PCR. For the ICW assay, infected confluent monolayers were fixed and permeabilized as described in methods, treated with different concentrations of chalcone **22** (1.0, 10 and 20 µg/mL) and successively incubated with anti-NP antibodies. At the same time, cell monolayers were stained with cell tag (a dye of cell proteins used for the normalization of viral protein expression).

The fluorescence intensity of NP (green) and cell tag (red) was measured by Odissey Imaging System. As reported in Figure 3 (Panel A), the NP expression was dose-dependently decreased on the concentration of **22** compared to untreated cells, suggesting the inhibition of the viral protein synthesis. Next, the expression of mRNAs for M2 was evaluated by RT PCR to evaluate the effect of chalcone in the early steps, such as the inhibition of viral RNA polymerase. As shown in Figure 3 (Panel B),

viral mRNAs normalized with GAPDH were dose-dependently decreased, and the percentage of viral titer calculated respect to untreated infected cells showed a reduction (about 84%) of viral mRNAs in cells treated with 10 µg/mL of **22**, confirming the inhibition at early stages of the virus life-cycle, probably during transcription or viral uncoating.

Table 5. IC50 values and selective index (SI) of stilbene derivatives **8–14**, **17–19** and chalcones **20–23**.

Entry	Compound	IC50 [a]	SI [b]
1	**8**	45.2	0.9
2	**9**	14.6	n.a. [c]
3	**10**	185.4	1.4
4	**11**	55	0.8
5	**12**	7.9	1.4
6	**13**	29.1	0.8
7	**14**	31.6	2.3
8	**17**	30.2	1.9
9	**18**	174	n.a.
10	**19**	n.a.	n.a.
11	**20**	29.7	1.1
12	**21**	37.1	0.4
13	**22**	9.5	4.4
14	**23**	24.5	1.5

[a] IC50 is the concentration (µg/mL) of inhibitor required to inhibit the antiviral activity by 50%. [b] SI is the ratio between cytotoxicity (CCA) and IC50. [c] n.a. values higher than 200 µg/mL.
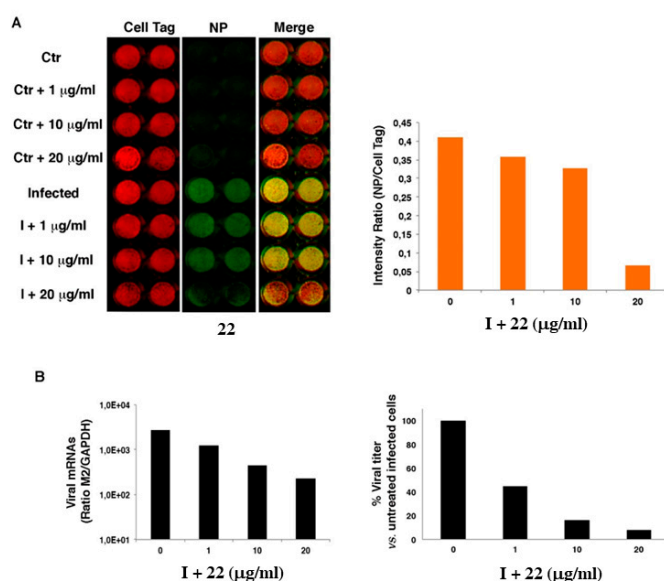

Figure 3. Mechanism of inhibition of influenza A virus replication by chalcone **22**. Panel (**A**) ICW assay on A549 cells infected with PR8. *Left panel*: The integrity of cell monolayer was revealed by Cell Tag on the 680 nm channel (red), viral NP expression on the 800 nm channel (green), merged images show the overlapping between viral protein and infected cells (yellow). *Right panel*. Fluorescence intensities were determined by the Odyssey software and green/red signal ratios were calculated and averaged for duplicate wells. Panel (**B**) Viral mRNAs for M2 were quantified by Real Time PCR on infected cell lysates at 24 h p.i. The housekeeping gene GAPDH was used for normalization. *Left panel*. Viral mRNAs ratios were calculated by using ΔΔCt method as described on methods. *Right panel*. The percentage (%) of viral titer was calculated respect to untreated infected cells (considered as 100%).

3. Materials and Methods

3.1. Materials

Eugenol (99%), 4-hydroxy-3-allylacetophenone (97%), 2-Methoxy-4-vinylphenol (98%), 4-Allyl-2,6-dimethoxyphenol (>95%), 2-Allylphenol (98%), 4-fluorobenzaldehyde (99%), allylamine (99.5%), 4-(allyloxy)benzaldehyde (99%), 4-hydroxy-benzaldehyde (98%), allylbromide (>98%), SBA-15 and, solvents EtOH (99.5%), Ethylacetate (99.5%) and CH_2Cl_2 (99.5%) were purchased from Sigma–Aldrich (Sigma-Aldrich, St. Louis, MO, USA), Aquamet-SIPr (99%) was purchased from Apeiron (Apeiron Synthesis S.A., Wrocław, Poland). ^{1}H NMR and ^{13}C NMR spectra were recorded on a Bruker (400 MHz) spectrometer (Bruker Italia S.r.l., Milan, Italy).

3.2. Catalyst Preparation

ASIPr/SBA-15 was prepared by applying the procedure reported in (BAlcar) in literature by Balcar et al. Briefly, SBA-15 (1.0 g) was dried in a Schlenk tube in vacuo at 300 °C for 3 h. Thereafter a solution of ASIPr (1.0 wt% of Ru) in 10 mL of CH_2Cl_2 was added dropwise under Argon atmosphere. After 20 min. the silica turned to slightly green and the solution became colorless. The solid was recovered by filtration on GH-polypro hydrophilic membranes (47 mm, 0.2 μm), washed with dry CH_2Cl_2 (3 × 10 mL) and dried under vacuum to yield ASIPr/SBA-15.

3.3. Textural Parameters

Textural parameters of SBA15 and ASIPr/SBA-15 were determined via a Micromeritics ASAP 2020 (Norcross, GA, USA), using nitrogen adsorption isotherms at 196 °C. Temperature program of method used: from 25 °C to 110 °C (0.5 °C/min) until the achievement of 1 Pa pressure. Samples were degassed by a turbomolecular pump vacuum for 10 h.

3.4. ICP–MS Analysis

The appropriate sample (from 1.0 mg to 10 mg) in fluorinated ethylene propylene (FEP) vials, was treated with regia solution. (750 μL HCl and 150 μL HNO_3) at 80° C for 3 h. Deionized water (4.0 mL) was added and then the sample was further diluted 10 times before the ICP–MS analysis (Agilent 7500 ICP–MS under clean room ISO6, Santa Clara, CA, USA).

3.5. Synthesis of Compounds **8**–**14**, **17**–**19** and **22**–**23**

Self-metathesis, olefin-metathesis and ring-closing metathesis of compounds 8–14, 17–19 and 22–23, respectively, were carried out by using similar experimental conditions. As a general procedure, the appropriate allyl and vinyl-benzene derivatives (0.6 mmol) were dissolved in dry CH_2Cl_2 (5.0 mL) in the presence of a catalytic amount of ASIPr/SBA-15 (2.0×10^{-3} mmol of immobilized Ru, corresponding to 8.8 mg of heterogenous catalyst)) under argon atmosphere at 40 °C for 4 h. Thereafter, the crude was filtered using GH-polypro hydrophilic membranes (47 mm 0.2 μm), concentrated at low pressure and purified by flash chromatography (Hexane/Etylacetate 4:1) to afford the desired products.

3.5.1. (E)-4,4'-(but-2-ene-1,4-diyl)bis(2-methoxyphenol) (**8**)

^{1}H-NMR (400 MHz, $CDCl_3$, ppm): δ 3.31 (d, *J* = 4 Hz, 4H, CH_2), 3.87–3.91 (overlapping singlets, 6H, CH_3), 5.71–5.87 (m, 2H, CH), 6.83–6.89 (m, 6Har, CH). ^{13}C-NMR (100 MHz, $CDCl_3$, ppm): δ (COCH$_3$), 146.8 (COH), 135.6 (CAr), 132.2 (C=C), 122.9 (CAr), 117.3 (CAr), 112.6 (CAr), 56.2 (CH$_3$), 41.1(CH$_2$). MS (ESI): *m/z* (M + H) + 301.34. Elemental Analysis for $C_{18}H_{20}O_4$ calculated: C, 71.98, H, 6.71, O, 21.31. Found: 71.95, H, 6.74, O, 21.25.

3.5.2. (E)-4,4'-(but-2-ene-1,4-diyl)bis(2,6-dimethoxyphenol) (**9**)

^{1}H-NMR (400 MHz, CDCl$_3$, ppm): δ 3.23–3.40 (m, 5.2 Hz, 4H, CH$_2$), 3.50–3.75 (overlapping singlets, 12H, CH$_3$), 5.56–5.70 (m, 2H, CH), 6.69 (s, 4Har, CH). ^{13}C-NMR (100 MHz, CDCl$_3$, ppm): δ (COCH$_3$), 136.2 (COH), 135.2 (CAr), 132.0 (C=C), 109.7 (CAr), 56.3 (CH$_3$), 40.1(CH$_2$). MS (ESI): *m/z* (M + H) + 361.16. Elemental Analysis for C$_{20}$H$_{24}$O$_6$ calculated: C, 66.65, H, 6.71, O, 26.63, Found: C, 66.62, H, 6.74, O, 25.93.

3.5.3. (E)-5,5'-(but-2-ene-1,4-diyl)bis(3-methoxybenzene-1,2-diol) (**10**)

^{1}H-NMR (400 MHz, CDCl$_3$, ppm): δ 3.32 (d, *J* = 4 Hz, 4H, CH$_2$), 3.81–3.95 (overlapping singlets, 6H, CH$_3$), 5.90–6.00 (m, 2H, CH), 6.71 (s, 2Har, CH), 6.79 (s, 2Har, CH). ^{13}C-NMR (100 MHz, CDCl$_3$, ppm): δ (COCH$_3$), 148.8 (COH), 136.2 (CAr), 132.4 (C=C), 125.4 (COH), 107.7 (CAr), 102.9 (CAr), 56.1 (CH$_3$), 39.8 (CH$_2$). MS (ESI): *m/z* (M + H) + 333.16. Elemental Analysis for C$_{18}$H$_{20}$O$_6$ calculated: C, 65.65, H, 6.07, O, 28.88. Found: C, 65.62, H, 6.04, O, 28.78.

3.5.4. (E)-1,1'-(but-2-ene-1,4-diylbis(4-hydroxy-3,1-phenylene))bis(ethan-1-one) (**11**)

^{1}H-NMR (400 MHz, CDCl$_3$, ppm): δ 3.40 (d, *J* = 4 Hz, 4H, CH$_2$), 5.89–6.00 (m, 2H, CH), 7.40 (d, 2Har, CH). 7.75 (d, 2Har, CH), 7.98 (overlapped singlets, 2Har, CH). ^{13}C-NMR (100 MHz, CDCl$_3$, ppm): δ (COCH$_3$), 159.8 (COH), 135.2 (CAr), 130.1 (C=C), 128.3 (CAr), 113.7 (CAr), 112.6 (CAr), 57.3 (CH$_3$), 40.3 (CH$_2$). MS (ESI): *m/z* (M + H) + 325.14. Elemental Analysis for C$_{20}$H$_{20}$O$_4$ calculated: C, 74.06, H, 6.22, O, 19.73. Found: C, 74.08, H, 6.24, O, 19.71.

3.5.5. (E)-2,2'-(but-2-ene-1,4-diyl)diphenol (**12**)

^{1}H-NMR (400 MHz, CDCl$_3$, ppm): δ 3.38 (d, *J* = 4 Hz, 4H, CH$_2$), 5.58-5.69 (m, 2H, CH), 6.71–6.79 (m, 4Har, CH), 6.97–7.10 (m, 4Har, CH). ^{13}C-NMR (100 MHz, CDCl$_3$, ppm): δ COH), 139.1 (CAr), 132.2 (CAr), 130.7 (C=C), 127.9 (CAr), 120.5 (CAr), 113.2 (CAr), 40.0 (CH$_2$). MS (ESI): *m/z* (M + H) + 241.12. Elemental Analysis for C$_{16}$H$_{16}$O$_2$ calculated: C, 79.97, H, 6.71, O, 13.32. Found: C, 79.95, H, 6.58, O, 13.31.

3.5.6. (E)-4,4'-(ethene-1,2-diyl)bis(2-methoxyphenol) (**13**)

^{1}H-NMR (400 MHz, CDCl$_3$, ppm): δ 3.89 (s, 6H, CH$_3$), 6.75 (d, *J* = 8 Hz, 2H, CH), 6.89 (d, *J* = 4, 2 Har, CH) 6.95 (d, *J* = 8 Hz, 2 Har, CH), 7.09 (s, 2Har, CH). ^{13}C-NMR (100 MHz, CDCl$_3$, ppm): δ (COCH$_3$), 146.2 (COH), 130.8 (CAr), 130.0 (C=C), 122.7 (CAr), 117.2 (CAr), 112.4 (CAr) 55.9 (CH$_3$). MS (ESI): *m/z* (M + H) + 273.10. Elemental Analysis for C$_{16}$H$_{16}$O$_4$ calculated: C, 70.58, H, 5.92, O, 23.50. Found: C, 70.58, H, 5.92, O, 23.50.

3.5.7. (E)-5,5'-(ethene-1,2-diyl)bis(3-methoxybenzene-1,2-diol) (**14**)

^{1}H-NMR (400 MHz, CDCl$_3$, ppm): δ 3.88 (s, 6H, CH$_3$), 6.70 (d, *J* = 8 Hz 2H, CH) 7.05 (overlapped singlets, 4Har, CH). ^{13}C-NMR (100 MHz, CDCl$_3$, ppm): δ (COCH$_3$), 145.5 (COH), 135.2 (COH), 133.3 (CAr), 130.8 (C=C), 107.4 (CAr), 105.2 (CAr), 55.8 (CH$_3$). MS (ESI): *m/z* (M + H) + 305.10. Elemental Analysis for C$_{16}$H$_{16}$O$_6$ calculated: C, 63.15, H, 5.30, O, 31.55. Found: C, 63.11, H, 5.28, O, 31.50.

3.5.8. (E)-5-(4-(4-hydroxy-3,5-dimethoxyphenyl)but-2-en-1-yl)-3-methoxybenzene-1,2-diol (**17**)

^{1}H-NMR (400 MHz, CDCl$_3$, ppm): δ 3.08 (10d, *J* =4 Hz, 4H, CH$_2$), 3.28 (s, 9H, CH$_3$), 5.78–5.89 (m, 2H, CH) 6.31 (s, 1H, Har, CH), 6.33 (s, 1H, Har, CH), 6.68 (overlapped singlets, 2 Har, CH). ^{13}C-NMR (100 MHz, CDCl$_3$, ppm): δ (COCH$_3$), (COCH$_3$), 146.2 (COH), 136.7 (CAr), 135.2 (CAr), 133.7 (CAr), 131.1 (C=C), 121.7 (CAr), 108.4 (CAr), 107.2 (CAr), 104.7 (CAr), 55.3 (CH$_3$), 39.5(CH$_2$). MS (ESI): *m/z* [M + H] + 347.14. Elemental Analysis for C$_{19}$H$_{22}$O$_6$ calculated: C, 65.88, H, 6.40, O, 27.71. Found: C, 65.84, H, 6.38, O, 27.68.

3.5.9. (E)-3-(4-(4-hydroxy-3, 5-dimethoxyphenyl)but-2-en-1-yl)benzene-1,2-diol (**18**)

^{1}H-NMR (400 MHz, CDCl$_3$, ppm): δ 3.30 (d, *J* = 4 Hz, 4H, CH$_2$), 3.90 (overlapped singlets, 6H, CH$_3$), 5.80–5.91 (m, 2H, CH) 6.52–6.63 (m, 3Har, CH) 6.80 (overlapped singlets, 2 Har, CH). ^{13}C-NMR (100 MHz, CDCl$_3$, ppm): δ (COCH$_3$), (COH), 145.3 (COH), 135.8 (CAr), 134.7 (CAr), 133.3 (CAr), 131.0 (C=C), 119.0 (CAr), 117.8 (CAr), 113.1 (CAr), 106.9 (CAr), 57.1 (CH$_3$), 38.2(CH$_2$), 37.8(CH$_2$). MS (ESI): *m/z* (M + H) + 317.14 Elemental Analysis for C$_{18}$H$_{20}$O$_5$ calculated: C, 68.34, H, 6.37, O, 25.29. Found: C, 68.28, H, 6.31, O, 25.20.

3.5.10. (E)-3-(4-(2-hydroxyphenyl)but-2-en-1-yl)benzene-1,2-diol (**19**)

^{1}H-NMR (400 MHz, CDCl$_3$, ppm): δ 3.39 (d, *J* = 4 Hz, 4H, CH$_2$), 5.88-5.99 (m, 2H, CH), 6.80-7.10 (m, 5Har, CH), 7.23-7.38 (m, 2Har, CH).^{13}C-NMR (100 MHz, CDCl$_3$, ppm): δ (COH), (COH), 145.3 (COH), 133.6 (CAr), 131.7 (CAr), 130.5 (C=C), 122.9 (CAr), 120.0 (CAr), 119.5 (CAr), 117.8 (CAr), 114.5 (CAr), 112.1 (CAr), 106.5 (CAr), 38.7(CH$_2$), 37.5 (CH$_2$). MS (ESI): *m/z* [M + H] + 257.11 Elemental Analysis for C$_{16}$H$_{16}$O$_3$ calculated: C, 74.98, H, 6.29, O, 18.73. Found: C, 74.95 H, 6.24, O, 18.71.

3.5.11. (3E,8E)-14-hydroxy-6-aza-1(1,3),5(1,4)-dibenzenacyclodecaphane-3,8-dien-2-one (**22**)

^{1}H-NMR (400 MHz, CD$_3$OD, ppm): δ 3.40 (d, *J* = 4 Hz, 2H, CH$_2$), 4.09 (d, *J* = 6 Hz, 2H, CH$_2$), 5.68-5.80 (m, 1H, CH), 6.12-6.26 (m, 1H, CH), 7.25 (d, *J* = 8 Hz, 1Har, CH), 7.52 (d, *J* = 6 Hz, 1H, CH), 7.70 (m, 2Har,1H, 3xCH) 7.88 (m, 3Har, CH), 7.98 (d, *J* = 8 Hz, 1Har, CH). ^{13}C-NMR (100 MHz, CD$_3$OD, ppm): δ (CO), (COH), 149.8 (CNH), 143.6 (C=C), 133.9 (CAr), 132.3 (CAr), 130.9 (CAr), 129.7 (CAr), 128.5 (CAr), 126.0 (C=C), 124.6 (C=C), 123.2 (C=C), 121.7 (CAr), 115.6 (CAr), 112.3 (CAr), 54.5 (CH$_2$), 32.1 (CH$_2$). MS (ESI): *m/z* (M + H) + 292.12 Elemental Analysis for C$_{19}$H$_{17}$NO$_2$ calculated C, 78.33, H, 5.88, N, 4.81, O, 10.98. Found: C, 78.29, H, 5.82, N, 4.71, O, 10.82.

3.5.12. (3E,8E)-14-hydroxy-6-oxa-1(1,3),5(1,4)-dibenzenacyclodecaphane-3,8-dien-2-one (**23**)

^{1}H-NMR (400 MHz, CD$_3$OD, ppm): δ 3.42 (dd, 2H, CH$_2$), 4.52 (d, *J* = 4 Hz, 2H, CH$_2$), 5.60–5.78 (m, 1H, CH), 6.10–6.20 (m, 1H, CH), 6.87 (d, *J* = 8 Hz, 1Har, CH), 6.91 (d, *J* = 8 Hz, 2Har, CH), 7.05 (d, *J* = 6 Hz, 1Har, CH), 7.50 (d, *J* = 8 Hz, 1Har, CH), 7.62–7.80 (m, 2Har, 1H, CH), 7.91 (s, 1H, CH). ^{13}C-NMR (100 MHz, CD$_3$OD, ppm): δ (CO), (COH), 159.8 (CO), 148.9 (C=C), 132.4 (CAr), 131.8 (CAr), 130.9 (CAr), 128.4 (CAr), 127.2 (CAr), 123.4 (C=C), 122.6 (C=C), 122.0 (C=C), 120.5 (CAr), 116.4 (CAr), 111.9 (CAr), 75.0 (CH$_2$), 35.5 (CH$_2$). MS (ESI): *m/z* (M + H) + 293.11 Elemental Analysis for C$_{19}$H$_{16}$O$_3$ calculated: C, 78.29, H, 5.82, N, 4.71, O, 10.82. Found: C, 77.89, H, 5.49, O, 16.39.

3.6. Synthesis of (E)-1-(3-allyl-4-hydroxyphenyl)-3-(4-(allylamino)phenyl)prop-2-en-1-one (20)

Chalcone 20 was prepared by nucleophilic aromatic displacement of previously prepared (E)-1-(3-allyl-4-hydroxyphenyl)-3-(4-fluorophenyl)prop-2-en-1-one (0.01 mol) with commercially available allylamine (0.05 mol). Reagents were dissolved in DMF(10 mL) and heated at 120 °C under magnetic stirring for 18 h in the presence of KOH (0.02 mol). Thereafter the mixture was cooled in ice bath, acidified with HCl 1N and extracted with ethyl acetate (3 × 50 mL). The aqueous phases were collected, basified with NaOH 1N and again extracted with ethyl acetate (3 × 50 mL). The organic phases were collected, concentrated at low pressure and the resulting brown oil purified by flash chromatography (hexane/ethylacetate 3:1) to afford the desired product 21 in quantitative yield.

^{1}H-NMR (400 MHz, CD$_3$OD, ppm): δ 3.46 (d, *J* = 6 Hz, 2H, CH$_2$), 4.12 (d, *J* = 4 Hz, 2H, CH$_2$), 4.98–5.10 (dd, 2H, CH), 5.18–5.36 (m, 2H, CH), 5.85–6.30 (m, 2H, CH), 7.48 (d, *J* = 8 Hz, 2Har, CH), 7.62 (m, 3H, CH), 7.78 (d, *J* = 6 Hz, 2Har, CH), 7.85 (d, *J* = 8, 1Har, CH), 7.91 (s, 1H, CH). ^{13}C-NMR (100 MHz, CD$_3$OD, ppm): δ (CO),(COH), 146.8 (CNH), 145.1 (C=C), 136.5 (C=C), 135.6 (C=C), 131.8 (CAr), 129.6 (CAr), 128.4 (CAr), 125.1 (CAr), 122.8 (CAr), 122.2 (CAr), 121.0 (C=C), 116.8 (C=C), 115.1 (C=C), 112.0 (CAr), 46.0 (CH$_2$), 35.7 (CH$_2$). MS (ESI): *m/z* [M + H] + 320.18 Elemental Analysis for C$_{21}$H$_{21}$NO$_2$ calculated: C, 78.97, H, 6.63, N, 4.39, O, 10.02. Found: C, 78.94, H, 6.57, N, 4.31, O, 9.82.

3.7. Synthesis of (E)-1-(3-allyl-4-hydroxyphenyl)-3-(4-fluorophenyl)prop-2-en-1-one

(*E*)-1-(3-allyl-4-hydroxyphenyl)-3-(4-fluorophenyl)prop-2-en-1-one was prepared by aldolic condensation between 4-hydroxy-3-allyl acetophenone (0.01 mol) and 4-fluorobenzaldehyde (0.011 mol) in EtOH under basic conditions (KOH, 0.02 mol) at 80 °C for 24 h. Thereafter the crude was neutralized with HCl 1N and extracted with ethylacetate (3×50 mL). The organic phases were collected and concentrated under reduced pressure. The dark brown solid obtained was recrystallized in MeOH to afford desired product as yellow solid in quantitative yield.

^{1}H-NMR (400 MHz, CD$_3$OD, ppm): δ 3.49 (d, *J* = 4 Hz, 2H,CH$_2$), 5.10–5.19 (m, 2H, CH$_2$), 6.02–6.10 (m, 1H, CH), 7.50 (d, *J* = 8 Hz, 2Har, CH), 7.62 (m, 3H, CH), 7.78 (d, *J* = 6 Hz, 2Har, CH), 7.85 (d, *J* = 8 (CO), (CF), (COH), 145.1 (C=C), 136.5 (C=C), 131.6 (CAr), 129.4 (CAr), 128.1 (CAr), 124.7 (CAr), 122.7 (CAr), 122.0 (CAr), 121.2 (C=C), 116.3 (CAr), 115.9 (C=C), 112.0 (CAr), 33.6 (CH$_2$). MS (ESI): *m/z* (M + H) + 283.11 Elemental Analysis for C$_{18}$H$_{15}$FO$_2$ calculated: C, 76.58, H, 5.36, F, 6.73, O, 11.33. Found: C, 76.49, H, 5.26, F, 6.51, O, 10.98.

3.8. Synthesis of Compound **21**

Chalcone 21 was prepared by aldolic condensation between 4-hydroxy-3-allyl acetophenone (0.01 mol) and 4-(allyloxy)benzaldehyde (0.011 mol) in EtOH under basic conditions (KOH, 0.02 mol) at 80 °C for 24 h. Thereafter the crude was neutralized with HCl 1N and extracted with etylacetate (3×50 mL). The organic phases were collected and concentrated under reduced pressure. The orange solid obtained was recrystallized in MeOH to afford desired product as yellow solid in quantitative yield.

^{1}H-NMR (400 MHz, CD$_3$OD, ppm): δ 3.42 (dd, 2H, CH$_2$), 4.52 (d, *J* = 4 Hz, 2H, CH$_2$), 5.05–5.10 (m, 2H, CH), 5.30–5.47 (m, 2H, CH), 5.90–6.20 (m, 2H, CH), 6.85 (d, *J* = 6 Hz, 1Har, CH), 6.90 (d, *J* = 8 Hz, 2Har, CH), 7.01 (d, *J* = 6 Hz, 1Har, CH), 7.48 (d, *J* = 8 Hz, 1Har, CH), 7.62–7.80 (m, 2HAr, 1H, CH), 7.91 (s, 1H, CH). ^{13}C-NMR (100 MHz, CD$_3$OD, ppm): δ (CO), (COH), 156.5 (CO), 145.3 (C=C), 136.9 (C=C), 136.2 (C=C), 133.8 (CAr), 131.5 (CAr), 128.7 (CAr), 128.4 (CAr), 125.1 (CAr), 122.8 (CAr), 122.2 (CAr), 121.0 (C=C), 115.2 (C=C), 114.1 (C=C), 113.0 (CAr), 70.1 (CH$_2$), 33.6 (CH$_2$). MS (ESI): *m/z* (M + H) + 321.14 Elemental Analysis for C$_{21}$H$_{20}$O$_3$ calculated C, 78.73, H, 6.29, O, 14.98. Found: C, 78.56, H, 6.21, O, 14.85.

3.9. Synthesis of 4-(Allyloxy)Benzaldehyde

Commercially available 4-hydroxy-benzaldehyde (0.01 mol) and allylbromide (0.011 mol) were dissolved in acetone (10 mL) and heated at 40 °C under magnetic stirring for 18 h in the presence of K$_2$CO$_3$ (0.02 mol). Thereafter the mixture was filtered, and extracted with ethyl acetate (3×50 mL). The organic phases were collected and concentrated under reduced pressure. The oil obtained was purified by flash chromatography (hexane/ ethylacetate 4:1) to afford the desired product in 75% of yield.

^{1}H-NMR (400 MHz, CDCl$_3$, ppm): δ 4.62 (d, *J* = 4 Hz, 2H, CH$_2$), 5.35–5.50 (dd, 2H, CH), 6.02–6.12 (m, 1H, CH), 7.02 (d, *J* = 6 Hz 2Har, CH), 7.85 (d, *J* = 6 Hz, 2Har, CH), 9.91 (s, 1H, CHO).

^{13}C-NMR (100 MHz, CDCl$_3$, ppm): δ (CO), (CO), 133.3 (C=C), 132.4 (CAr), 129.1(CAr), 118.0 (C=C), 114.5 (CAr), 70.2 (CH$_2$). MS (ESI): *m/z* (M + H) + 163.08 Elemental Analysis for C$_{10}$H$_{10}$O$_2$ calculated C, 74.06, H, 6.22, O, 19.73. Found: C, 74.00, H, 6.11, O, 19.62.

3.10. Evaluation of Antioxidant Activity by DPPH Assay

The compounds were dissolved in EtOH with a final different concentration (500, 250, 100, 50, and 10 μg/mL) and 0.5 mL of DPPH (6.0×10^{-5} M in EtOH) were added on. Mixture were stirred for 15 s and incubated at room temperature for 30 min. The change in the colour was measured using Shimadzu UV-3600 UV/VIS spectrophotometer (Japan, Kyoto) at 518 nm until the reaction reached a plateau and ethanol was used as a blank. The radical scavenging activity was determined with using the Equation (1). The kinetic of the process was analyzed for each concentration tested and the rate of

DPPH remaining at the steady state was estimated. This value was used to calculate the IC 50 (defined as the concentration of substrate μg/mL that causes 50% loss of DPPH activity).

3.11. Virus Production and Infection

Allantoic cavities of 10-day-old embryonated chicken eggs used to growth influenza virus A/Puerto Rico/8/34 H1N1 (48 h at 37 °C), were harvested and centrifuged (5000 rpm, 30 min). The recovered virus, was used for the infection of A549 epithelial cells (confluent monolayers epithelial were challenged for 1 h at 37 °C) at a multiplicity of infection (m.o.i.) of 0.0001. At the end the cells have been washed with PBS, and further incubated with a supplemented medium (2% FCS). Allantoic fluid from uninfected eggs was used as reference for mock infection.

3.12. Haemagglutination (HAU) Assay

Hemagglutinin units (HAU) were evaluated (24 h post infection) in human type 0 Rh+ erythrocytes. The appropriate sample in DMSO (highest concentration in the culture medium value equal to 0.2%) was diluted with deionized water in RPMI (1, 10, 20 and 50 μg/mL) and added after the adsorption period to the culture media. The treatment of cells with DMSO alone was used as reference.

3.13. In Cell Western (ICW) Assay

The ICW assay was performed using the Odyssey Imaging System (LI-COR, Lincoln, NE) as described in reference 51. A549 cells grown in 96-well plates (2×10^4 cells/well), either infected or mock-infected (Ctr) with PR8, were fixed with 4% formaldeyde, washed, permeabilized with 0.1% Triton X-100 and incubated with PBS containing Odyssey Blocking buffer (LI-COR Biosciences, Lincoln, NE). The cells were then stained at 4 °C overnight with mouse anti-NP (1:400, Santa Cruz Biotechnology) together with Cell Tag (1:2000, LI-COR Biosciences, Lincoln, NE) in PBS containing 5% Odyssey Blocking Buffer. Cells were then washed and stained with goat anti-mouse IRDyeTM 800 antibody (1:3000, LI-COR Biosciences, Lincoln, NE). Protein expression was quantified using the Odyssey Imaging System. For statistical analysis, integrated intensities of fluorescence in wells were determined using software provided with the imager station (LI-COR). The relative amount of NP protein was obtained by normalizing to the Cell Tag in all experiments.

3.14. RT-PCR

Total RNA was extracted from pellet of infected cells by means of Total RNA Purification Plus Kit (Norgen Bioteck corp.) for RT-PCR. Complementary DNA (cDNA) was synthesized with iScriptcDNA Synthesis Kit (BioRad), which have blend of oligo (dT) and random primers. PCR was composed by cDNA, IQ™ SYBR® Green Supermix fluorophore, and following primers for Matrix protein M2: forward, 5′-GCAAGCATGAGAACCATTGG-3′, and reverse, 5′-GCGGCAATAGCGAGAGGATC-3′. As an endogenous control, the following primers for GAPDH were used: forward, 5′-CTCCCCACACACATGCACTTA-3′, and reverse, 5′-CCTAGTC CCAGGGCTTTGATT-3′. The relative amount of target mRNA ($2^{-\Delta\Delta Ct}$) was obtained by normalizing to the endogenous GAPDH reference in all experiments.

4. Conclusions

ASIPr/SBA-15 was an efficient heterogeneous catalyst for the synthesis of stilbene and chalcone derivatives by different type of metathesis procedures. As a general trend, self-metathesis and cross-metathesis afforded products in yield higher than ring-closing metathesis. Conversion of substrate from 27% to 95%, and yield of product from 15% to 75%, were obtained depending on the structural properties of the reagents. Irrespective from the experimental conditions, the presence of electro-donating OH group in the *ortho*-position of the aromatic ring with respect to the olefin side-chain appreciably decreased the yield of the reaction, while the highest yield in the self-metathesis

were obtained reducing the length of the olefin side-chain. Noteworthy, ASIPr/SBA-15 showed a reactivity similar to ASIPr in all of the types of reactions studied. ASIPr/SBA-15 was stable enough for six successive runs, showing only a slight decrease in the conversion of substrate and yield of product, associated to a low leaching of the ruthenium active species. Two of the novel stilbene derivatives and one macrocyclic chalcone showed appreciable IC50 values in the inhibition of influenza A virus on A549 cells, the chalcone being characterized by the highest value of selectivity index. In this latter case, studies on the expression of viral nucleoprotein (NP) and viral RNA expression suggested the occurrence of the inhibition at early stages of the virus life-cycle, probably during transcription or viral uncoating.

References

1. Shaw, M.L.; Palese, P. Orthomyxoviridae: The Viruses and Their Replication. In *Fields Virology*, 6th ed.; Knipe, D.M., Howley, P.M., Eds.; Lippincott Williams & Wilkins: Philadelphia, PA, USA, 2013; pp. 1648–1698.

2. Go, Y.-M.; Kang, S.-M.; Roede, J.R.; Orr, M.; Jones, D.P. Increased Inflammatory Signaling and Lethality of Influenza H1N1 by Nuclear Thioredoxin-1. *PLoS ONE* **2011**, *6*, e18918. [CrossRef] [PubMed]

3. Nencioni, L.; Aquilano, K.; Cozzolino, F.; Garaci, E.; Palamara, A.T.; Iuvara, A.; Ciriolo, M.R.; Rotilio, G. Influenza A virus replication is dependent on an antioxidant pathway that involves GSH and Bcl-2. *FASEB J.* **2003**, *17*, 758–760. [CrossRef] [PubMed]

4. Gannagé, M.; Dormann, D.; Albrecht, R.; Dengjel, J.; Torossi, T.; Rämer, P.C.; Lee, M.; Strowig, T.; Arrey, F.; Conenello, G.; et al. Matrix protein 2 of influenza A virus blocks autophagosome fusion with lysosomes. *Cell Host Microbe* **2009**, *6*, 367–380. [CrossRef] [PubMed]

5. Kim, C.U.; Lew, W.; Williams, M.A.; Liu, H.; Zhang, L.; Swaminathan, S.; Bischofberger, N.; Chen, M.S.; Mendel, D.B.; Tai, C.Y.; et al. Influenza Neuraminidase Inhibitors Possessing a Novel Hydrophobic Interaction in the Enzyme Active Site: Design, Synthesis, and Structural Analysis of Carbocyclic Sialic Acid Analogues with Potent Anti-Influenza Activity. *J. Am. Chem. Soc.* **1997**, *119*, 681–690. [CrossRef]

6. Sgarbanti, R.; Amatore, D.; Celestino, I.; Marcocci, M.E.; Fraternale, A.; Ciriolo, M.R.; Magnani, M.; Saladino, R.; Garaci, E.; Palamara, A.T.; et al. Intracellular redox state as target for anti-influenza therapy: Are antioxidants always effective? *Curr. Top. Med. Chem.* **2014**, *14*, 2529–2541. [CrossRef] [PubMed]

7. Chong, J.; Poutaraud, A.; Hugueney, P. Metabolism and roles of stilbenes in plants. *Plant Sci.* **2009**, *177*, 143–155. [CrossRef]

8. Jian, W.; He, D.; Song, S. Synthesis, Biological Evaluation and Molecular Modeling Studies of New Oxadiazole-Stilbene Hybrids against Phytopathogenic Fungi. *Sci. Rep.* **2016**, *6*, 31045. [CrossRef]

9. Mahboub, R.; Memmou, F. Antioxidant activity and kinetics studies of eugenol and 6-bromoeugenol. *Nat. Prod. Res.* **2014**, *29*, 966–971. [CrossRef]

10. Rimando, A.; Suh, N. Biological/Chemopreventive Activity of Stilbenes and their Effect on Colon Cancer. *Planta Med.* **2008**, *74*, 1635–1643. [CrossRef]

11. Li, X.; Dai, Y.; Yan, S.; Shi, Y.; Li, J.; Liu, J.; Cha, L.; Mu, J. Resveratrol lowers blood pressure in spontaneously hypertensive rats via calcium-dependent endothelial NO production. *Clin. Exp. Hypertens.* **2016**, *38*, 1–7. [CrossRef]

12. Zhang, Y. Pterostilbene, a novel natural plant conduct, inhibits high fat induced atherosclerosis inflammation via nf-κb signaling pathway in toll-like receptor 5(tlr5) deficient mice. *Biomed. Pharmacother.* **2016**, *81*, 345–355. [CrossRef] [PubMed]

13. Su, Q.; Pu, H.; Hu, C. Neuroprotection by combination of resveratrol and enriched environment against ischemic brain injury in rats. *Neurol. Res.* **2016**, *38*, 60–68. [CrossRef] [PubMed]

14. Baile, C.A.; Yang, J.-Y.; Rayalam, S.; Hartzell, D.L.; Lai, C.-Y.; Andersen, C.; Della-Fera, M.A.; Della-Fera, M.A. Effect of resveratrol on fat mobilization. *Ann. N. Y. Acad. Sci.* **2011**, *1215*, 40–47. [CrossRef] [PubMed]

15. Wong, R.; Nealon, R.; Scholey, A.; Howe, P. Low dose resveratrol improves cerebrovascular function in type 2 diabetes mellitus. *Nutr. Metab. Cardiovasc. Dis.* **2016**, *26*, 393–399. [CrossRef] [PubMed]

16. Chalal, M.; Klinguer, A.; Echairi, A.; Meunier, P.; Vervandier-Fasseur, D.; Adrian, M. Antimicrobial Activity of Resveratrol Analogues. *Molecules* **2014**, *19*, 7679–7688. [CrossRef] [PubMed]

17. Kosuru, R.; Rai, U.; Prakash, S.; Singh, A.; Singh, S. Promising therapeutic potential of pterostilbene and its mechanistic insight based on preclinical evidence. *Eur. J. Pharmacol.* **2016**, *789*, 229–243. [CrossRef]

18. Campagna, M.; Rivas, C. Antiviral activity of resveratrol. *Biochem. Soc. Trans.* **2010**, *38*, 50–53. [CrossRef]

19. Benencia, F.; Courrèges, M.C. In vitro and in vivo activity of eugenol on human herpesvirus. *Phytother. Res.* **2000**, *14*, 495500. [CrossRef]

20. Liu, T.; Zang, N.; Zhou, N.; Li, W.; Xie, X.; Deng, Y.; Ren, L.; Long, X.; Li, S.; Zhou, L.; et al. Resveratrol Inhibits the TRIF-Dependent Pathway by Upregulating Sterile Alpha and Armadillo Motif Protein, Contributing to Anti-Inflammatory Effects after Respiratory Syncytial Virus Infection. *J. Virol.* **2014**, *88*, 4229–4236. [CrossRef]

21. Heredia, A.; Davis, C.; Amin, M.N.; Le, N.M.; Wainberg, M.A.; Oliveira, M.; Deeks, S.G.; Wang, L.-X.; Redfield, R.R. Targeting host nucleotide biosynthesis with resveratrol inhibits emtricitabine-resistant HIV-1. *AIDS* **2014**, *28*, 317–323. [CrossRef]

22. Zhang, L.; Li, Y.; Gu, Z.; Wang, Y.; Shi, M.; Ji, Y.; Sun, J.; Xu, X.; Zhang, L.; Jiang, J.; et al. Resveratrol Inhibits Enterovirus 71 Replication and Pro-Inflammatory Cytokine Secretion in Rhabdosarcoma Cells through Blocking IKKs/NF-κB Signaling Pathway. *PLoS ONE* **2015**, *10*, 116879. [CrossRef] [PubMed]

23. Nakamura, M.; Saito, H.; Ikeda, M.; Hokari, R.; Kato, N.; Hibi, T.; Miura, S. An antioxidant resveratrol significantly enhanced replication of hepatitis C virus. *World J. Gastroenterol.* **2010**, *16*, 184–192. [CrossRef] [PubMed]

24. Aquilano, K.; Hernandez, L.; Cozzolino, F.; Palamara, A.T.; Nencioni, L.; De Chiara, G.; Ciriolo, M.R.; Garaci, E. Inhibition of Influenza A Virus Replication by Resveratrol. *J. Infect. Dis.* **2005**, *191*, 1719–1729.

25. Grubbs, R.H. *Handbook of Metathesis*, 1st ed.; Wiley-VCH: Weinheim, Germany, 2003; ISBN 978-3-527-30616-9.

26. Grubbs, R.H.; Trnka, T.M. Ruthenium-Catalyzed Olefin Metathesis. In *Ruthenium in Organic Synthesis*; Murahashi, S., Ed.; Wiley-VCH: Weinheim, Germany, 2004; pp. 153–177.

27. Bilel, H.; Hamdi, N.; Zagrouba, F.; Fischmeister, C.; Bruneau, C. Eugenol as a renewable feedstock for the production of polyfunctional alkenes via olefin cross-metathesis. *RSC Adv.* **2012**, *2*, 9584. [CrossRef]

28. Blackwell, H.E.; O'Leary, D.J.; Chatterjee, A.K.; Washenfelder, R.A.; Bussmann, D.A.; Grubbs, R.H. New approaches to olefin cross-metathesis. *J. Am. Chem. Soc.* **2000**, *122*, 58–71. [CrossRef]

29. Vieille-Petit, L.; Clavier, H.; Linden, A.; Blumentritt, S.; Nolan, S.P.; Dorta, R. Ruthenium olefin metathesis catalysts with N-heterocyclic carbene ligands bearing n-naphthyl side chains. *Organometallics* **2010**, *29*, 775. [CrossRef]

30. De Souza, T.B.; De Oliveira Brito, K.M.; Silva, N.C.; Rocha, R.P.; De Sousa, G.F.; Duarte, L.P.; Coelho LF, L.; Dias AL, T.; Veloso, M.P.; Carvalho, D.T.; et al. New Eugenol Glucoside-Based Derivative Shows Fungistatic and Fungicidal Activity against Opportunistic Candida Glabrata. *Chem. Biol. Drug Des.* **2016**, *87*, 83–90. [CrossRef]

31. Broggi, J.; Urbina-Blanco, C.A.; Clavier, H.; Leitgeb, A.; Slugovc, C.; Slawin AM, Z.; Nolan, S.P. The Influence of Phosphane Ligands on the Versatility of Ruthenium–Indenylidene Complexes in Metathesis. *Chem. Eur. J.* **2010**, *16*, 9215. [CrossRef]

32. Moıse, J.; Arseniyadis, S.; Cossy, J. Cross-Metathesis between α-Methylene-γ-butyrolactone and Olefins: A Dramatic Additive Effect. *Org. Lett.* **2007**, *9*, 1695–1698. [CrossRef]

33. Harvey, B.G.; Sahagun, C.M.; Guenthner, A.J.; Groshens, T.J.; Cambrea, L.R.; Reams, J.T.; Mabry, J.M. A High-Performance Renewable Thermosetting Resin Derived from Eugenol. *ChemSusChem* **2014**, *7*, 1964–1969. [CrossRef]

34. Hasib-Ur-Rahman, M.; Belkacemi, K.; Hamoudi, S. Heterogeneous olefin-metathesis: Comparative perspective of the activity with respect to unsaturated fatty acid methyl esters. *Can. J. Chem. Eng.* **2017**, *95*, 1850–1863. [CrossRef]

35. Suriboot, J.; Bazzi, H.S.; Bergbreiter, D.E. Supported Catalysts Useful in Ring-Closing Metathesis, Cross Metathesis, and Ring-Opening Metathesis Polymerization. *Polymers* **2016**, *8*, 140. [CrossRef] [PubMed]

36. Öztürk, B.G. Ammonium tagged Hoveyda-Grubbs catalysts immobilized on magnetically separable core-shell silica supports for ring-closing metathesis reactions. *Microporous Mesoporous Mater.* **2018**, *267*, 249–256. [CrossRef]

37. Bhar, S.; Ananthakrishnan, R. Ru(ii)-Metal complex immobilized mesoporous SBA-15 hybrid for visible light induced photooxidation of chlorophenolic compounds in aqueous medium. *Photochem. Photobiol. Sci.* **2017**, *16*, 1290–1300. [CrossRef] [PubMed]

38. Zhao, D.; Sun, J.; Li, Q.; Stucky, G.D. Morphological Control of Highly Ordered Mesoporous Silica SBA-15. *Chem. Mater.* **2000**, *12*, 275–279. [CrossRef]

39. Pastva, J.; Skowerski, K.; Czarnocki, S.J.; Žilková, N.; Čejka, J.; Bastl, Z.; Balcar, H. Ru-Based Complexes with Quaternary Ammonium Tags Immobilized on Mesoporous Silica as Olefin Metathesis Catalysts. *ACS Catal.* **2014**, *4*, 3227–3236. [CrossRef]

40. Balcar, H.; Čejka, J. Mesoporous molecular sieves as advanced supports for olefin metathesis catalysts. *Coord. Chem. Rev.* **2013**, *257*, 3107–3124. [CrossRef]

41. Liao, Z.-H.; Hsu, P.-W.; Hung, T.-C.; Liao, G.-J.; Chern, Z.-Y.; Lai, Y.-L.; Yu, L.-C.; Hsu, Y.-J.; Wang, J.-H.; Chen, P.; et al. Investigation of Thermal Stability and Reactivity of Rh Nanoclusters on an Ultrathin Alumina Film. *Catalysts* **2019**, *9*, 971. [CrossRef]

42. Balcar, H.; Žilková, N.; Kubů, M.; Polášek, M.; Zedník, J. Metathesis of cardanol over ammonium tagged Hoveyda-Grubbs type catalyst supported on SBA-15. *Catal. Today* **2018**, *304*, 127–134. [CrossRef]

43. Delaude, L.; Demonceau, A.; Noels, A.F.; Ferré-Filmon, K.; Ferre-Filmon, K. Stereoselective Synthesis of (E)-Hydroxystilbenoids by Ruthenium-Catalyzed Cross-Metathesis. *Eur. J. Org. Chem.* **2005**, *2005*, 3319–3325.

44. Krzysztof, S.; Lukasz, G.; Micha, B.; Czarnocki, S.; Szczepaniak, G.; Wierzbicka, C. (4-((4-Ethyl-4-methylpiperazin-1-ium-1-yl)methyl)-1,3-dimesitylimidazolidin-2 ylidene)dichloro(2-isopropoxybenzylidene)ruthenium(II) chloride. Patent Number PCT/EP2013/053967, 6 September 2013.

45. Bannin, T.J.; Datta, P.P.; Kiesewetter, E.T.; Kiesewetter, M.K. Synthesizing Stilbene by Olefin Metathesis Reaction Using Guided Inquiry to Compare and Contrast Wittig and Metathesis Methodologies. *J. Chem. Educ.* **2019**, *96*, 143–147. [CrossRef]

46. Lo, C.H.; Cariou, R.; Fischmeister, C.; Dixneufa, P.H. Styrene Initiators. *Arab. J. Chem.* **2016**, *9*, 931–935.

47. Fioravanti, R.; Celestino, I.; Costi, R.; Crucitti, G.C.; Pescatori, L.; Mattiello, L.; Novellino, E.; Checconi, P.; Palamara, A.T.; Nencioni, L.; et al. Effects of polyphenol compounds on influenza A virus replication and definition of their mechanism of action. *Bioorganic Med. Chem.* **2012**, *20*, 5046–5052. [CrossRef] [PubMed]

48. Siatka, T.; Kašparová, M. Seasonal Variation in Total Phenolic and Flavonoid Contents and DPPH Scavenging Activity of Bellis perennis L. Flowers. *Molecules* **2010**, *15*, 9450–9461. [CrossRef]

49. Bizzarri, B.M.; Botta, L.; Capecchi, E.; Celestino, I.; Checconi, P.; Palamara, A.T.; Nencioni, L.; Saladino, R. Regioselective IBX-Mediated Synthesis of Coumarin Derivatives with Antioxidant and Anti-influenza Activities. *J. Nat. Prod.* **2017**, *80*, 3247–3254. [CrossRef]

50. Fujisawa, S.; Murakami, Y. *Eugenol and Its Role in Chronic Diseases*; Springer Science and Business Media LLC: Berlin, Germany, 2016; Volume 929, pp. 45–66.

51. Wan, Y.; Zhou, Z.; Yang, Y.; Wang, J.; Hung, T. Application of an In-Cell Western assay for measurement of influenza A virus replication. *J. Virol. Methods* **2010**, *169*, 359–364. [CrossRef]